



Contents lists available at ScienceDirect

Saudi Pharmaceutical Journal

journal homepage: www.sciencedirect.com



Original article

## Cubic liquid crystalline nanoparticles containing a polysaccharide from *Ulva fasciata* with potent antihyperlipidaemic activity

Azza A. Matloub<sup>a</sup>, Mona M. AbouSamra<sup>b,\*</sup>, Alaa H. Salama<sup>b</sup>, Maha Z. Rizk<sup>c</sup>, Hanan F. Aly<sup>c</sup>, Ghada Ibrahim Fouad<sup>c</sup>

<sup>a</sup> Pharmacognosy Department, National Research Centre, Cairo, Egypt

<sup>b</sup> Pharmaceutical Technology Department, National Research Centre, Cairo, Egypt

<sup>c</sup> Therapeutic Chemistry Department, National Research Centre, Cairo, Egypt

### ARTICLE INFO

#### Article history:

Received 31 October 2017

Accepted 5 December 2017

Available online 7 December 2017

#### Keywords:

*Ulva fasciata*

Polysaccharide

Cubic liquid crystalline nanoparticle

Antihyperlipidaemic

Cubosomes

### ABSTRACT

The present study involves the preparation of cubic liquid crystalline nanoparticles (cubosomes) for liver targeting to assess the potential of a formulated bioactive polysaccharide isolated from the hot aqueous extract of *Ulva fasciata* as an alternative natural agent with anti-hyperlipidaemic activity. Cubosomal nanoparticles were prepared by disrupting the cubic gel phase of the polysaccharide and water in the presence of a surfactant. Different lipid matrices and stabilizers were tested. All the formulations were in the nanosize range and showed sufficient negative charge to inhibit the aggregation of the cubosomes. Drug entrapment efficiencies (EEs%) were determined and in vitro release studies were performed. Transmission electron microscopy (TEM) and differential scanning calorimetry were used to analyze the loaded cubosomal nanoparticles containing glyceryl monostearate (GMO 2.25 g), poloxamer 407 (0.25 g) and 50 mg of the polysaccharide. A preclinical study comparing the cubic liquid crystalline nanoparticles containing polysaccharide to *fluvastatin* as a reference drug in hyperlipidaemic rats was conducted. The rats treated with the polysaccharide-loaded cubosomes showed significant decreases in total cholesterol (TC), triglycerides (TG) and total lipid (TL) compared to the untreated HL rats. In addition, oxidative stress and antioxidant biomarkers were measured in the HL rats. Compared to the untreated HL rats, the cubosome treated rats showed a significant reduction in malondialdehyde (MDA), whereas insignificant changes were detected in nitric oxide (NO), glutathione (GSH) levels and total antioxidant capacity (TAC). Further, vascular and intercellular adhesion molecules (VCAM, ICAM), and myeloperoxidase were demonstrated. A histopathological examination was conducted to study the alterations in histopathological lesions and to document the biochemical results. In conclusion, this study demonstrates the superiority of using a natural lipid regulator such as polysaccharide loaded cubosomes instead of *fluvastatin*.

© 2017 The Authors. Production and hosting by Elsevier B.V. on behalf of King Saud University. This is an open access article under the CC BY-NC-ND license (<http://creativecommons.org/licenses/by-nc-nd/4.0/>).

### 1. Introduction

One of the most important goals in the pharmaceutical industry is targeting drugs to specific organs and tissues. In this context, the

search for new drug delivery approaches and new modes of action represents one of the main challenges at present. The advances necessary to improve the therapeutic index and bioavailability of systems capable of site-specific delivery require a multidisciplinary scientific approach (Haag and Kratz, 2006; Korting and Schafer-Korting, 2010; Semete et al., 2010; Wang et al., 2011). With the increased usage of nanotechnology, nanomedicine has emerged as a strategy for the production of commercially available drug products. Nanomedicine involves the innovative use of nanometer scale materials to develop new approaches and therapies. Because of their characteristic small size, surface structure and high surface area, materials exhibit unique physicochemical properties (Semete et al., 2010). Such properties facilitate the intracellular uptake of nanomaterials to specific cellular targets, helping overcome the current limitations of traditional formulations.

\* Corresponding author at: Pharmaceutical Technology Department, National Research Centre, 33 El-Buhouth Street, Dokki, Giza 12622, Egypt.

E-mail addresses: [m\\_mona14@hotmail.com](mailto:m_mona14@hotmail.com), [mm.samra@nrc.sci.eg](mailto:mm.samra@nrc.sci.eg) (M.M. AbouSamra).

Peer review under responsibility of King Saud University.



Production and hosting by Elsevier

Fatty liver disease is a reversible condition where large vacuoles of triglyceride fat accumulate in liver cells via the process of steatosis (i.e. abnormal retention of lipids within a cell). Fat accumulation may be accompanied by a progressive inflammation of the liver (hepatitis), i.e., steatohepatitis (Katiyar et al., 2016). In a previous study performed in our lab, we proved that a polysaccharide from *Ulva fasciata* polysaccharide was an effective anti-hyperlipidaemic agent (Matloub et al., 2013; Borai et al., 2015; Rizk et al., 2016a, 2016b). Polysaccharides a family of active materials similar to sialic acid; enhances the negative charges on cell surfaces to affect the aggregation of cholesterol in the blood, thereby, decreasing serum cholesterol levels (Li et al., 2008).

Cubic liquid crystals, also known as cubosomes, are dispersed nanostructured particles characterized by high biocompatibility and bioadhesive properties (Spicer, 2005). Cubosomes are produced in a liquid crystalline phase with cubic crystallographic symmetry and are formed by the self-assembly of amphiphilic or surfactant like molecules (Scriven, 1976). However, the cubic phases possess the unique property of very high solid like viscosity: because of their interesting bicontinuous structures, which enclose two distinct regions of water separated by a controlled bilayer of surfactant (Rizwan et al., 2007). Consequently, the cubic phases can be fractured and dispersed to form particulate dispersions that are colloidal and thermodynamically stable for a long time (Scriven, 1976). Cubosomes are characterized by their capability to encapsulate hydrophilic, hydrophobic and amphiphilic substances (Gustafsson et al., 1997; Bei et al., 2010). They also enable targeted and controlled drug release (Bei et al., 2010) and easily prepared and low cost.

This work describes a simple method for preparing a cubic phase gel matrix containing the polysaccharide isolated from the hot aqueous extract of *Ulva fasciata*. The prepared cubic gel matrix could be dispersed in water to form cubosomal nanoparticle dispersion prior to oral administration.

The polysaccharide-loaded cubosomes were evaluated for their *in vitro* and *in vivo* characteristics to explore their potential as a targeted drug delivery system providing optimal concentration of polysaccharide to the liver tissues.

## 2. Materials

The polysaccharide was isolated from the hot aqueous extract of *Ulva fasciata* as described by Matloub et al. (2013). Glycerol mono-oleate (GMO), glycerol mono-stearate (GMS), poloxamer 407 and poloxamer 188 were purchased from Sigma-Aldrich Chemical Company (Milwaukee, USA). Cellulose membrane dialysis tubing (molecular weight cut-off of 12,000–14,000 g/mole); was purchased from Sigma-Aldrich Chemical Company; St. Louis, USA. Fluvastatin was purchased from NOVARTIS Pharmaceuticals (Egypt, Cairo). Enzyme-linked immunosorbption assay (ELISA) kits were provided by UCSN (U.S.A.) for myeloperoxidase (MPO) and Eiaab (USA) for both vascular cell adhesion molecule-1 (VCAM-1) and soluble intracellular adhesion molecule-1 (ICAM-1). Other chemicals and reagents were purchased from Biodiagnostic Company for Diagnostic and Research Reagents; (Egypt). All solvents and reagents were of analytical grades.

## 3. Methodology

### 3.1. Acquisition of the extract calibration curve using the sulfuric acid-UV method

The procedure for the proposed sulfuric Acid-UV method is as follows. A 1 ml aliquot of carbohydrate solution was rapidly mixed with 3 ml of concentrated sulfuric acid in a test tube and vortexed

for 30 s. The temperature of the mixture increases rapidly within 10–15 s after the addition of sulfuric acid. Then, the solution was cooled on ice for 2 min to bring it to room temperature. Finally, the UV light absorption of the sample was read using a UV spectrophotometer (Shimadzu UV spectrophotometer 2410/PC, Japan) at 322 nm. Reference solutions were prepared according to the same procedure described above, except that the carbohydrate aliquot was replaced with distilled water (Albalasmeh et al., 2013).

### 3.2. Preparation of blank and drug-loaded cubic gels

For a blank cubic gel, GMO or GMS (2.25 g) and poloxamer 407 (0.25 g) or poloxamer 188 (0.25 g) were melted at 70 °C in a water bath. The obtained molten solution was added dropwise to 4 ml of deionized water (70 °C) and vortexed. The solution was mixed at high speed at room temperature to achieve a homogenous state. The mixture was equilibrated at room temperature for 48 h to obtain the blank cubic gel (Nasr et al., 2015). The drug-loaded cubic gel was prepared by dissolving 50 or 100 mg of extract in 4 ml of deionized water before adding the GMO or GMS/poloxamer 407 or poloxamer 188 molten solutions. The prepared formulations were subjected to physical examination to identify the homogeneous gel and the separated system. The remaining steps were the same steps as those described for the preparation of the blank cubic gel. The cubic gels were stored at ambient temperature until use.

### 3.3. Preparation of cubosomal nanoparticles dispersions

To prepare the cubosomal dispersions, the cubic gel was dispersed in 18.50 ml of deionized water by vortexing at high speed for 3 min. The final concentration of lipids in the dispersion was 10% (w/w) with respect to the final dispersion weight. The final extract concentration in the cubosomal dispersion was 2 mg/g cubosomal dispersion.

### 3.4. Characterization of cubosomes

#### 3.4.1. Particle size

The average diameter of the cubosomal dispersions and polydispersity index (PDI) were determined by photon correlation spectroscopy (PCS) using a Zetasizer Nano ZS (Malvern Instruments, Malvern, UK) at a fixed angle of 90° and at 25 °C. The aqueous cubosomal dispersions were diluted with distilled water before analysis. Each value represents the average of 3 measurements.

#### 3.4.2. Zeta potential analysis

The particle charge was quantified as zeta potential (ZP) using a Zetasizer Nano ZS (Malvern Instruments, Malvern, UK) at 25 °C. Before measuring, each sample had to be diluted with demineralized particle free water to reach an adequate intensity. Each measurement was performed at least in triplicate.

### 3.5. Determination of drug entrapment efficiency and drug loading capacity

The entrapment efficiency (E.E.) was determined by measuring the concentration of drug in the supernatant after centrifugation using a cooling centrifuge (Union 32R, Korea). The untrapped drug was determined by adding 1 ml of drug-loaded cubic gel to 9 ml of water and then centrifuging this dispersion at 9000 rpm and 4 °C for 30 min. The supernatant was collected, filtered through a Millipore membrane filter (0.2 μm), then diluted with water and measured using the sulfuric-acid-UV method against a blank. The E.E. was calculated using the following equation (Hou et al., 2003; Souto et al., 2004):

$$E.E.\% = \frac{\text{Initial drug conc.} - \text{free drug conc.}}{\text{Initial drug conc.}} \times 100$$

The drug loading capacity (D.L.%) was calculated according to the following equation:

$$D.L.\% = \frac{\text{Amount of entrapped drug}}{\text{Drug nanoparticle weight}} \times 100$$

### 3.6. *In vitro* drug release studies

The *in vitro* release of polysaccharide from the different cubosomal dispersions was evaluated by the dialysis bag diffusion method reported by Yang et al. (2000). The release studies were performed in phosphate buffer at pH 6.8. Polysaccharide-loaded cubosomal dispersions equivalent to 2 mg of drug were suspended in distilled water (donor compartment) in a dialysis bag (molecular weight cut-off of 12,000–14,000 g/mol) sealed at both ends and dialysed against phosphate buffer (receptor compartment). The dialysis bag was immersed in the receptor compartment containing 50 ml of dissolution medium, which was stirred at 100 rpm and maintained at  $37 \pm 2$  °C. The receptor compartment was covered to prevent evaporation of the dissolution medium. To determine the amount of drug that diffused through the dialysis bag, samples (2 ml) were taken from the receptor compartment and the same amount of fresh dissolution medium was added to keep a constant volume at fixed time points (0.5, 1, 2, 3, 4, 5, and 6 h). The polysaccharide in the samples was measured spectrophotometrically at 322 nm. The release studies were carried out in triplicate for all formulations, and the results were expressed as the mean values  $\pm$  SD. The cumulative percent of polysaccharide released was plotted against time.

### 3.7. Transmission electron microscopy

The morphology of the selected cubosomal formulation was evaluated using a transmission electron microscope (TEM, JEOL JEM1230, Tokyo, Japan). One drop of diluted sample was placed on a copper grid and stained with 2% (w/v) phosphotungstic acid for examination. The experiment was conducted at room temperature, and micrograph was taken at a suitable magnification power.

### 3.8. Differential scanning calorimetry

To detect any possible change in the physical state of the polysaccharide in the cubic gel, differential scanning calorimetry (DSC) was performed on the drug-loaded cubic gel, blank cubic gel, polysaccharide and poloxamer 407 using a thermal analysis system (DSC-60, Shimadzu, Japan). The samples (5 mg) were heated from 25 to 400 °C at a constant rate of 10 °C/min in an aluminium pan under a nitrogen atmosphere. The thermograms obtained were evaluated for peak shifts or the appearance/disappearance of new peaks.

## 3.9. Assay of antihyperlipidaemic activity

### 3.9.1. Preparation of animals

Sixty male Wister rats ( $120 \pm 10$  gm), were provided by the animal house of the National Research Centre (NRC). These rats were housed in a temperature-controlled environment (26–29 °C) with a fixed light/dark cycle for two weeks as an adaptation period and were supplied with water and food *ad libitum*. The present study was approved by the Ethical Committee of the NRC, Egypt (16,047).

**3.9.1.1. Induction of hyperlipidaemia.** Rats were fed orally with a high-fat diet (composed of lard mixed with a normal diet in a ratio of 1:5 for twelve consecutive weeks according to Adaramoye et al. (2008) to establish the rat model of hyperlipidaemia. The lipid profile of total cholesterol (TC), triglycerides (TG) and total lipids (TL) was determined for selected HL rats.

### 3.9.2. Experimental design

Rats were randomly divided into four groups of 15 rats each as follows:

**Group 1:** Served as a normal control (fed with a normal diet and distilled water). The normal diet was composed of yellow corn, soybean meal, extruded soybean seed, corn gluten, limestone powder, mono-calcium phosphate, L-lysine hydrochloride, salt, sodium bicarbonate, a mixture of vitamins and minerals, D- & L-methionine and choline chloride.

**Group 2:** Served as the HL rats.

**Group 3:** HL rats that received an oral dose of 100 mg/kg.b.wt (dose was inoculated using a gastric tube) of formulated hot polysaccharide extract-loaded cubosomes. This dose was calculated based on the therapeutic dose for rats (Pengzhan et al., 2003).

**Group 4:** HL rats that received an oral dose of 2 mg/kg.b.wt. of *fluvastatin*. This dose was calculated based on the therapeutic dose (10 mg/day) for human beings (Koter et al., 2002) using the conversion table of Paget and Barnes (Paget and Barnes, 1964).

The normal groups continued to be provided with the common commercial rat chow. All treatments were given orally 5 times/week for 4 weeks.

### 3.9.3. Collection of blood samples

At the end of the experiment, the animals were withheld food for at least 12 h, and venous blood samples were collected by puncture of the sublingual vein into sterilized tubes for serum separation and were immediately centrifuged at 3000 rpm for 15 min at 4 °C. Next, the clear, non haemolyzed supernatant sera were quickly removed and frozen at –20 °C until biochemical measurements of the lipid profile, liver function parameters, inflammatory myeloperoxidase (MPO), nitric oxide (NO) and cell adhesion molecules; vascular and intercellular adhesion molecules (CAMs, i.e., VCAM-1 and ICAM-1).

### 3.9.4. Biochemical examination

**3.9.4.1. Lipid profile.** Serum was used to determine the levels of TC, TG and TL with colourimetric methods (Zollner and Kirsch, 1962; Allain et al., 1974; Fossati and Prencipe, 1982).

### 3.9.4.2. Endothelial dysfunction markers.

**3.9.4.2.1. Nitric oxide.** Serum nitric oxide (NO) was determined according to the method of Montgomery and Dymock (1986).

**3.9.4.2.2. Cell adhesion molecules.** Rat soluble intercellular adhesion molecule-1 (s-ICAM-1) and rat soluble vascular cell adhesion molecule-1 (s-VCAM-1); concentrations were determined using **ELISA**.

**3.9.4.2.3. Inflammatory markers.** *In vivo* quantitative measurements of MPO were performed using ELISA. The results were expressed as the mean  $\pm$  SD and the differences between groups were compared statistically using Student's *t* test and Co-state statistical software, different letters were used to denote significant differences at  $p \leq .05$ .

## 3.10. Histopathological examination of processed liver samples

Liver biopsies were fixed in 10% buffered formalin, and were processed until embedded in paraffin. Serial liver sections with a thickness of 4  $\mu$ m were obtained from the prepared paraffin blocks. The liver sections were stained with haematoxylin and eosin.

Histopathological examination of the stained sections was conducted using a Zeiss microscope (Drury and Wallington, 1980).

### 3.11. Statistical analysis

Statistical analysis was accomplished using SPSS® software (USA). Comparison between two or more groups was conducted using the unpaired *t* test or one-way analysis of variance (ANOVA) followed by the least significant difference test, respectively. A *p* values < .05 was considered statistically significant.

## 4. Results and discussion

### 4.1. Preparation of cubosomal nanoparticles

The polysaccharide-loaded cubosomal nanoparticles were composed of GMO or GMS (2.25 g), and were stabilized by 0.25 g of surfactant (poloxamer 188 or poloxamer 407). The polysaccharide was incorporated at different concentrations (50 and 100 mg).

Eight formulations were prepared, and; the composition of the investigated cubosomal formulations is shown in Table 1. The prepared formulations were evaluated visually as a homogenous gel or as two separated systems. All the formulations containing GMS were found to exhibit phase separation. By contrast, when GMO was used, an opalescent dispersion of the cubic nanoparticles was obtained. This observation can be attributed to the unsaturated double bond present in the GMO which may help its interaction with the drug. On the other hand, the GMS is a saturated compound; so no chance for interaction occurrence with other components. This suggestion may explain the phase separation in the GMS formulations' compared to homogeneity in case of GMO formulations'. The four selected formulations containing GMO were subjected to further investigations.

### 4.2. Characterization of the prepared cubosomal vesicles

#### 4.2.1. Particle size and zeta potential analysis

The particle size (PS), PDI and ZP results are presented in Table 1. All the formulations were in the nanoscale range, with sizes between  $255 \pm 9.11$  and  $588.6 \pm 14.23$  nm. The results showed an increase in the PS with increasing drug concentration (CUB-F1 & CUB-F2 versus CUB-F3 & CUB-F4). This observation can be explained by the assumption that the lipid has a certain loading capacity and that the addition of excess drug can lead to aggregation, yielding a larger PS. The size distributions of polysaccharide cubosomal dispersions were monomodal. The relatively low PDI values as showed in Table 1 are proving the formation of almost homogenous nanoparticles in the preparations.

As well, the ZP values showed the presence of sufficient charge to inhibit aggregation of cubosomes via electric repulsion, indicating that the formulations are stable.

### 4.3. Drug entrapment efficiency and drug loading capacity

The E.Es of all the formulations are presented in Table 1. It can be observed the high E.Es values for the prepared formulations which can be largely due to the presence of GMO which is a commonly used oil in drug delivery that can also act as an emulsifying agent (Basha et al., 2017). To evaluate the effect of the different formulation variables on the drug E.E., entrapment factors including the type and concentration of surfactant and the concentration of the drug were studied. The acquired data showed that increasing the concentration of the *Ulva* polysaccharide from 50 mg to 100 mg, resulted in a significant decrease ( $p < .05$ ) in the entrapment efficiency and loading capacity of the tested polysaccharide in the cubosomal formulations (CUB-F1 & CUB-F2 versus CUB-F3 & CUB-F4). This decrease can be attributed to the fact that the amount of drug added had increased above the encapsulation capacity of GMO (Salama and Aburahma, 2016). Therefore, many drug molecules remained unencapsulated at a drug concentration of 100 mg. Regarding the effect of the surfactant type, formulations containing poloxamer 407 showed higher E.Es and loading capacity than those containing poloxamer 188 with the same amount of drug (CUB-F1 & CUB-F3; CUB-F2 & CUB-F4). This result was in agreement with many studies showing that poloxamer 407 is the stabilizer of choice in cubosome preparation (Spicer, 2005; Rizwan et al., 2007; Nasr et al., 2015). Furthermore, the low hydrophilic lipophilic balance (HLB) of poloxamer 407 compared to that of poloxamer 188 contributed to the high drug entrapment efficiency. It was reported that incorporation of surfactants with low HLB values during the preparation of nonionic vesicles significantly increase the E.E. (Rizwan et al., 2007). The results reveal that the highest E.E. ( $67.3 \pm 2.65\%$ ) and drug loading capacity ( $25.1 \pm 0.3$ ) were achieved in the cubosomal formulation CUB-F1 as shown in Table 1.

### 4.4. In vitro drug release study

The results of investigating in vitro drug release from the loaded cubosomes are presented in Fig. 1. The relatively slow release of the active compound observed from the cubosomes may be attributed to the limited diffusion of the drug molecules incorporated in the aqueous channels; in this case diffusion is governed by the tortuosity and the relatively narrow pore size of the aqueous channels (Anderson and Wennerstroem, 1990; Clogston et al., 2005). The potential of cubosomes to serve as a slow release matrix for drugs of varying sizes and polarities has been reported (Burrows et al., 1994; Sadhale and Shah, 1999; Lara et al., 2005; Shah and Paradkar, 2005; Clogston et al., 2005; Nguyen et al., 2011). Another factor contributing to the slow drug release from the cubosomes is the presence of GMO as one of their main components, which might lead to slower partitioning of the drug from the oily medium to the aqueous one (Nguyen et al., 2011).

**Table 1**  
Composition of different cubosomal gel (CUB) formulations.

Formula	Lipid	Surfactants (gm)		Polysaccharide Conc. (mg)	P.S (nm ± S.D.)	Z.P (mV ± S.D.)	PDI	E.E.%	D.L.%
		Poloxamer 407	Poloxamer 188						
CUB-F1	GMO	0.25	–	50	$255 \pm 9.1$	$-22.3 \pm 1.3$	$0.24 \pm 0.3$	$67.3 \pm 2.6$	$25.1 \pm 0.3$
CUB-F2		0.25	–	100	$498.8 \pm 22.3$	$-16.7 \pm 0.6$	$0.33 \pm 0.02$	$55.3 \pm 3.5$	$15.3 \pm 0.2$
CUB-F3		–	0.25	50	$272.3 \pm 9.2$	$-25.2 \pm 1.2$	$0.27 \pm 0.01$	$57.1 \pm 1.5$	$10.4 \pm 1.1$
CUB-F4		–	0.25	100	$588.6 \pm 14.2$	$-16.7 \pm 0.5$	$0.31 \pm 0.4$	$50.0 \pm 3.7$	$12.1 \pm 0.4$
CUB-F5	GMS	0.25	–	50	–	–	–	–	–
CUB-F6		0.25	–	100	–	–	–	–	–
CUB-F7		–	0.25	50	–	–	–	–	–
CUB-F8		–	0.25	100	–	–	–	–	–

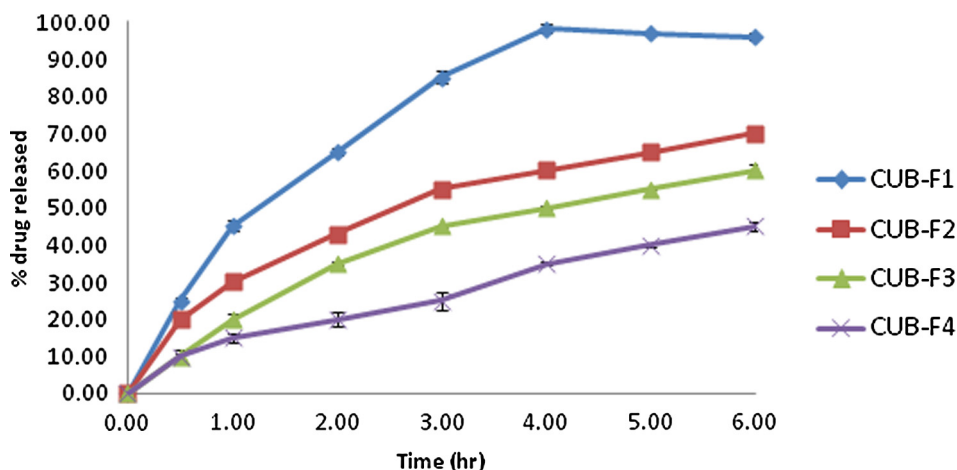


Fig. 1. *In-vitro* drug release profiles of the prepared cubosomal formulations (n = 3) in phosphate buffer saline (pH 6.8).

#### 4.5. Characterization of the optimized cubosomal vesicles

As shown in the results presented above, the cubosomal formulation CUB-F1 exhibited the highest E.E., a high negative ZP and the smallest PS. Thus, it was selected for characterization by TEM and DSC analysis and *in vivo* investigations.

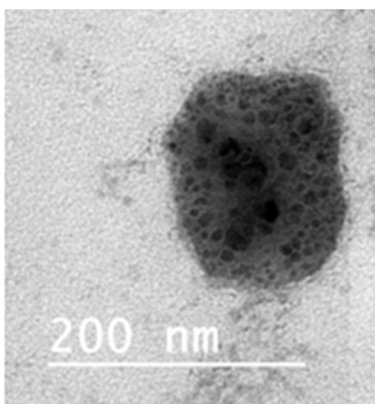


Fig. 2. TEM photograph of the drug loaded cubosomal vesicle CUB-F1.

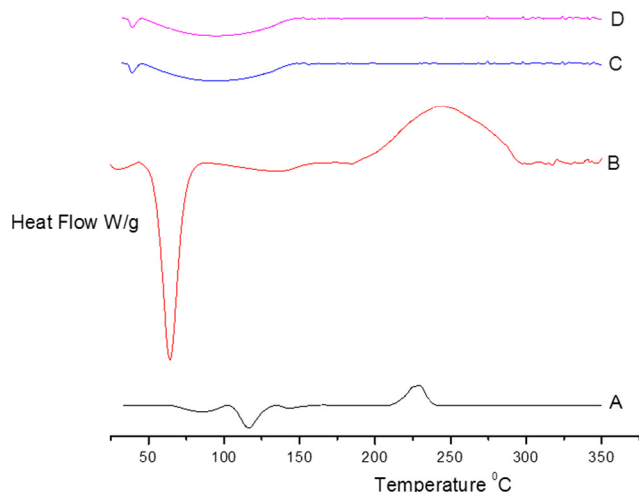


Fig. 3. DSC thermograms of (A) polysaccharide, (B) poloxamer 407 (C), blank cubosome and (D) CUB-F1.

#### 4.5.1. Transmission electron microscopy

The morphological examination of the drug-loaded cubosomal formulation CUB-F1 was performed using TEM. Fig. 2 reveals that the tested formulation was cubic in shape. It has been previously reported that using poloxamer 407 in colloidal nano-vesicles can alter their spherical shape into cubic shape (Salama et al., 2016). Moreover the particle diameters measured by TEM were noticeably smaller than those determined by the Zeta sizer. This result can be explained by the dehydration of particles due to drying during the TEM analysis.

#### 4.5.2. Differential scanning calorimetry

Fig. 3 shows the DSC thermograms of the polysaccharide, poloxamer 407, blank cubosome and CUB-F1. The thermogram of the polysaccharide showed an endothermic melting peak at approximately 122.5 °C. By contrast, the thermogram of CUB-F1 showed complete disappearance of the melting peak of the drug which indicates the formation of an amorphous dispersion of the drug in the prepared cubosome (AbouSamra and Salama, 2017).

#### 4.6. Assay of antihyperlipidaemic activity

The results from the measurements of the serum lipid profile, liver function parameters, and inflammatory marker (MPO) and CAM (VCAM-1 and ICAM-1) levels are revealed in Tables 2 and 3. Table 2 shows that compared to the normal rats, the TC, TG and TL levels in HL rats significantly increased by 63.58, 92.51 and 88.85%, respectively. Treatment of HL rats with CUB-F1 caused a significant decrease in TC, TG, and TL levels compared to the untreated HL rats, with percentages of improvement of 55.82, 44.26 and 77.49%, respectively. However, fluvastatin recorded higher percentages of improvement for TC, TG and TL than CUB-F1 (55.96, 56.60 and 78.89%, respectively). Furthermore, feeding the rats with a high-fat (i.e., cholesterol-enriched) diet for 12 weeks resulted in a dramatic rise in serum TC, TG and TL levels. These results are consistent with those reported by Jang et al. (2008), who declared that the high level of LDL-C found in HL rats may be attributed to a down-regulation of LDL receptors by the cholesterol and saturated fatty acids included in the diet (Flock et al., 2011).

Therefore, treatment of HL rats with the formulated polysaccharide from *Ulva fasciata* induced a significant and marked decrease in serum TL levels.

Table 2 indicates that compared to the normal control rats, the malondialdehyde (MDA) and NO levels in HL rats significantly increased by 39.57 and 42.99%, respectively, whereas, the

**Table 2**

Effect of CUB-F1 supplementation on serum lipid profile, oxidative stress and antioxidant biomarkers in HL rats.

Biomarkers/Groups	Serum lipid profile				Oxidative stress and antioxidant biomarkers			
	Parameters	TC (mg/dl)	TG (mg/dl)	TL (mg/dl)	MDA (mg/dl)	NO ( $\mu$ mol/l)	GSH (mg/dl)	TAC (Mm/l)
Negative control rats	Mean $\pm$ SD	60.58 $\pm$ 9.98 <sup>a</sup>	40.47 $\pm$ 4.18 <sup>a</sup>	1000.30 $\pm$ 16.23 <sup>a</sup>	8.34 $\pm$ 0.99 <sup>a</sup>	13.98 $\pm$ 0.79 <sup>a</sup>	72.79 $\pm$ 4.56 <sup>a</sup>	1.88 $\pm$ 0.10 <sup>a</sup>
Hyperlipidemic rats (HL)	Mean $\pm$ SD	99.10 $\pm$ 5.12 <sup>b</sup>	77.91 $\pm$ 3.28 <sup>b</sup>	1889.13 $\pm$ 17.22 <sup>b</sup>	11.64 $\pm$ 1.00 <sup>b</sup>	19.99 $\pm$ 1.22 <sup>b</sup>	49.4 $\pm$ 3.66 <sup>b</sup>	0.945 $\pm$ 0.06 <sup>b</sup>
	% change to C	+63.58	+92.51	+88.85	6.89 $\pm$ 0.94 <sup>c</sup>	12.86 $\pm$ 1.09 <sup>a</sup>	66.33 $\pm$ 10.28 <sup>a</sup>	1.495 $\pm$ 0.08 <sup>a</sup>
CUB-F1 treated rats	Mean $\pm$ SD	67.105 $\pm$ 7.90 <sup>a</sup>	60.00 $\pm$ 8.22 <sup>c</sup>	1113.96 $\pm$ 16.23 <sup>a</sup>	–17.39	–8.01	–8.87	–20.48
	% change to C	+10.76	+48.26	+11.36	–40.80	–35.66	+34.27	+58.20
	% change to HL	–32.29	–22.98	–41.03	56.95	51.00	23.26	29.26
	%improvement	52.82	44.26	77.49	7.00 $\pm$ 0.67 <sup>c</sup>	12.09 $\pm$ 1.09 <sup>a</sup>	66.00 $\pm$ 7.44 <sup>a</sup>	1.38 $\pm$ 0.09 <sup>a</sup>
HL-Fluvastatin treated rats	Mean $\pm$ SD	65.20 $\pm$ 5.40 <sup>a</sup>	55.00 $\pm$ 4.13 <sup>c</sup>	1099.91 $\pm$ 10.00 <sup>a</sup>	–16.07	–13.52	–9.33	–26.59
	% change to C	+7.62	+35.90	+9.95	–39.86	39.52	+33.60	+46.03
	% change to HL	–34.20	–29.40	–41.77	55.63	56.51	22.81	23.14
	%improvement	55.96	56.60	78.89	6.89 $\pm$ 0.94 <sup>c</sup>	12.86 $\pm$ 1.09 <sup>a</sup>	66.33 $\pm$ 10.28 <sup>a</sup>	1.495 $\pm$ 0.08 <sup>a</sup>

TC: Total cholesterol, TG: Total triglyceride, TL: Total lipids, MDA: Malondialdehyde, NO: Nitric Oxide, GSH: Glutathione reduced, TAC: Total antioxidant capacity. Data represented as mean  $\pm$  SD of ten rats in each group. Statistical analysis is carried out using SPSS computer program, (one way analysis of variance), coupled with co-state computer program. Superscript unshared letters are significant at  $P < .05$ , where similar letters are considered insignificant at  $P > .05$ . These are statistical results.

**Table 3**

Effect of CUB-F1 supplementation on ICAM, VCAM and MPO levels in HL rats.

Biomarkers/Groups	Parameters	ICAM (ng/ml)	VCAM (ng/ml)	MPO(Pg/ml)
Negative control rats	Mean $\pm$ S.D.	4.99 $\pm$ 0.05 <sup>a</sup>	12161.36 $\pm$ 65.43 <sup>a</sup>	120.90 $\pm$ 5.20 <sup>a</sup>
Hyperlipidemic rats (HL)	Mean $\pm$ S.D.	17.27 $\pm$ 0.91 <sup>b</sup>	15311.05 $\pm$ 62.22 <sup>b</sup>	178.59 $\pm$ 13.10 <sup>b</sup>
	% change	+246.09	+25.89	+47.72
CUB-F1 treated rats	Mean $\pm$ S.D.	7.93 $\pm$ 0.85 <sup>c</sup>	13044.19 $\pm$ 43.09 <sup>a</sup>	133.52 $\pm$ 10.10 <sup>c</sup>
	% change to C	+58.92	+7.26	+10.44
	% change to HL	–54.08	–14.81	–25.24
	% improvement	187.17	18.64	37.28
HL-Fluvastatin treated rats	Mean $\pm$ S.D.	8.22 $\pm$ 0.53 <sup>a</sup>	12533.43 $\pm$ 52.09 <sup>a</sup>	125.50 $\pm$ 9.59 <sup>c</sup>
	% change to control	$\pm$ 64.73	3.10	+3.80
	% Change to HL	–52.40	–18.14	–29.73
	% improvement	181.36	22.84	43.91

(VCAM-1): Vascular cellular adhesion molecule-1, (ICAM-1): Intercellular adhesion molecule-1. MPO: myeloperoxidase. Data presented Data represented as mean  $\pm$  SD of ten rats in each group. Statistical analysis is carried out using SPSS computer program, (one way analysis of variance), coupled with co-state computer program. Superscript unshared letters are significant  $P < .05$ , where similar letters are considered insignificant at  $P > .05$ . These are statistical results.

glutathione (GSH) and total antioxidant capacity (TAC) levels were significantly reduced by 32.13 and 49.73%, respectively. Treatment of HL rats with the formulated polysaccharide from *Ulva fasciata* (CUB-F1) caused a significant reduction in MDA with a percentage of improvement of 56.95%. However, insignificant changes were detected in the NO, GSH and TAC levels of the HL rats compared to the normal control rats. Furthermore, the drug loaded formulation CUB-F1 induced a higher percentage of improvement in oxidative stress and antioxidant biomarkers than *fluvastatin* (Table 2). Oxidative stress is one of the main mechanisms of action of hypercholesterolemia. Excess lipid accumulation in the liver can damage bio-membranes and the mitochondrial respiratory chain and increase  $\beta$ -oxidation of fatty acids, which in turn; leads to an imbalance in oxidative phosphorylation and the formation of free radicals. Oxidative stress also causes liver damage by inducing numerous reactive and cytotoxic intermediate products that subsequently leads to cell necrosis or apoptosis. In addition, oxidative stress produces an inflammatory reaction through cell injury, causing infiltration of the liver parenchyma by inflammatory cells (Rizk et al., 2016b). The results of our study showed that supplementation of HL rats with the formulated CUB-F1 modulated antioxidant activities and lipid peroxide levels in the liver. The depletion of GSH and TAC is associated with an increase in lipid peroxidation, and a decrease in GSH level may also result from enhanced utilization of the tested drug by the antioxidant enzymes; glutathione peroxidase and glutathione-S-transferase (Rizk et al., 2016a).

Table 3 shows that compared with the normal control rats, the ICAM and VCAM levels in HL rats significantly increased by 16.66 and 25.89%, respectively. However, rats treated with either CUB-F1 or *fluvastatin* exhibited insignificant changes in both ICAM and VCAM levels compared to the control group. Nevertheless, compared to the untreated HL rats, CUB-F1 as well as *fluvastatin* elicited a significant decrease in both CAMs. Ustvol et al. (2017) found a correlation between adhesion molecules and fatty liver patients and observed high serum levels of ICAM-1 and VCAM-1 in patient with fatty liver disease compared to healthy control patients. Based on the data presented in Table 3, CUB-F1 was inhibited the expression of VCAM-1 and ICAM-1, which is known to have a protective effect against the progression of atherosclerosis (Han et al., 2017).

Moreover, the study revealed that the HL-rats exhibited strong activation of MPO, which is implicated in pathophysiological alterations, and may become a crucial mediator accelerating the progression of inflammatory disease during hyperlipidaemia. In accordance with our results, Yida et al. reported marked elevation in inflammatory markers levels in HL rats and methodically linked this elevation to the risk of atherosclerosis (Yida et al., 2015). Compared to atherogenic rats, HL rats treated with CUB-F1 showed a noticeable and significant decrease in the atherogenic inflammatory marker MPO, which might be due to the direct inhibition of MPO expression. Inducing rats with hypercholesterolemia led to over-induction of ICAM-1 and VCAM-1.

High glucose and oxidized LDL-C levels are the main contributing factors to oxidative stress, and VCAM-1 and ICAM-1 activation. Both CAMs caused monocytes activation, and upon moving to the subendothelial layer, they promote vascular diseases (Blankenberg et al., 2003). CUB-F1 was found to suppress VCAM-1/ICAM-1, which is considered to have therapeutic potential against cardiovascular diseases (CVDs). The observed decrease in the number of adhesion molecules may also be attributed to antioxidative effects of CUB-F1 that decrease the oxidation of LDL-C to ox-LDL-C (Rizk et al., 2016a).

Interestingly, CUB-F1 showed increased antihyperlipidaemic activity compared with fluvastatin as a reference drug (Table 4). It is important to note that fluvastatin has induced many side effects, especially in hepatic tissue; these side effects include elevated values in liver function tests (1.1%). Persistent elevations in liver function parameters of three times over normal values were reported in up to 1.1% of patients administered fluvastatin in clinical trials. This finding led to the discontinuation of fluvastatin in 0.7% of patients (Langtry and Markham, 1999). By contrast, the hot polysaccharide extract could protect the liver from fulminant damage (Said et al., 2017) indicating that CUB-F1 could be used safely as a natural lipid regulator in place of fluvastatin (Table 2). Since, CUB-F1 treated HL rats showed high improvement percentages reached to 56.95, 51.00, 23.26 and 29.26%, for MDA, NO, GSH

and TAC respectively in comparison with fluvastatin which recorded 55.63, 56.51, 22.81 and 23.14%, respectively

#### 4.7. Histopathological examination

Histopathological examination of liver biopsies from the normal control rats clearly showed the normal histological structure of the hepatic lobule (Fig. 4A). However, the livers of the positive control rats showed congestion of the central veins (Fig. 4B) and hydropic degeneration of hepatocytes (Fig. 4C). Meanwhile, the livers of rats from the treated group exhibited congestion of hepatic sinusoids and Kupffer cells activation (Fig. 4D&E). In good agreement with the present findings, Rizk et al. found numerous swollen liver cells and hydropic degeneration in HL rats (Rizk et al., 2016b). Different sizes of fat droplets and fatty degeneration of the liver were observed in the cytoplasm of hepatocytes from the HL rats. An inflammatory cell infiltration along with spotty and patchy necrosis of hepatocytes was also observed in the lobule and portal areas. In the present study, histological investigations showed that the HL rats displayed important lipid droplet accumulation and that treatment with the formulated polysaccharide dramatically reduced the number of hepatocytes containing lipid droplets. Lipid droplets were previously observed in only the liver tissue of HL rats (Suanarunsawat et al., 2011), which could be attributed to lipid accumulation in the hepatocyte cytoplasm. Oxidized LDL induces the expression of scavenger receptors on the macrophage surface. These scavenger receptors promote the accumulation of modified lipoproteins, forming an early atheroma (Alam et al., 2011). In addition, administration with the formulated extract as well as the drug fluvastatin induced liver recovery, including decreased signs of fatty liver disease with less congestion and Kupffer cells activation.

#### 5. Conclusion

Cubic liquid crystalline nanoparticles loaded *Ulva fasciata* polysaccharide was effectively prepared. Selected formulation chosen according to high E.E. and drug loading capacity, small particle size and high release efficiency was subjected to a preclinical study against hyperlipidaemic rats compared to fluvastatin as a reference

**Table 4**  
Relative antihyperlipidemic biomarkers activity of CUB-F1 to fluvastatin drug.

Biomarkers	Relative%
TC	94.42
TG	78.16
Total Lipids	98.23
GSH	101.99
TAC	126.44
MDA	102.35
NO	90.23
ICAM	95.91
VCAM	81.64
MAO	84.89

Activity > 75% high, 75–50%: good, 50–25%: normal, <25%: weak activity.

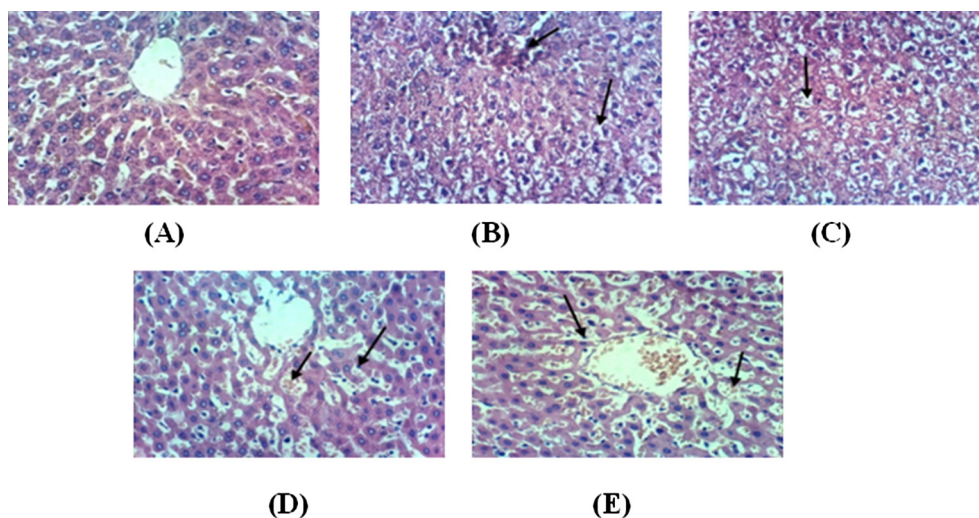


**Fig. 4.** Histopathological sections of rats' liver (A) Liver of control, untreated rat showing the normal histological structure of hepatic lobule (H & E X 400), (B) Liver of hyperlipidemic positive rat showing congestion of central vein and hydropic degeneration of hepatocytes (H & E X 400). Many cells show eccentric nucleus with fat deposition, (C) Liver of control positive rat showing hydropic degeneration of hepatocytes (H & E X 400). Many cells show eccentric nucleus with fat deposition, (D) Treated group with CUB-F1 showing congestion of hepatic sinusoids and Kupffer cells activation (H & E X 400), (E) Liver of rat from treated standard fluvastatin-HC group showing congestion of hepatic sinusoids and Kupffer cells activation (H & E X 400).

drug. CUBF1 showed superiority as a natural lipid regulator compared with *fluvastatin*. Such result can be an excellent and safe addition in the field of pharmaceuticals for effective treatment of hyperlipidaemia.

### Acknowledgements

The authors acknowledge financial support from the National Research Centre – Egypt through a grant (No: 10010204).

### Conflict of interest

The authors declare that there are no conflicts of interest.

### References

- AbouSamra, M.M., Salama, A.H., 2017. Enhancement of the topical tolnaftate delivery for the treatment of tinea pedis via provesicular gel systems. *J. Liposome Res.* 27 (4), 324–334.
- Adaramoye, O., Akinatyo, O., Achen, J., Michel, A., 2008. Lipid-lowering effects of methanolic extracts of *Vernonia anagydalina* leaves in rats fed on high cholesterol diet. *Vasc. Health Risk Manage.* 4 (1), 235–241.
- Alam, N., Yoon, K.N., Lee, T.S., Lee, U.Y., 2011. Hypolipidemic activities of dietary Pleurotusostreatus hypercholesterolemic rats. *Mycobiology* 39, 45–51.
- Albalasmeh, A.A., Berhe, A.A., Ghezzehei, T.A., 2013. A new method for rapid determination of carbohydrate and total carbon concentrations using UV spectrophotometry. *Carbohydr. Polym.* 97 (2), 253–261.
- Allain, C.C., Poon, L.S., Chan, C.S., Richmond, W., Fu, P.C., 1974. Enzymatic determination of total serum cholesterol. *Clin. Chem.* 20 (4), 470–475.
- Anderson, D.M., Wennerstroem, H., 1990. Self-diffusion in bicontinuous cubic phases, L3 phases, and microemulsions. *J. Phys. Chem.* 94, 8683–8693.
- Basha, M., Salama, A.H., El Awdan, S., 2017. Reconstitutable spray dried ultra-fine dispersion as a robust platform for effective oral delivery of an antihyperlipidemic drug. *Int. J. Pharmaceut.* 532, 478–490.
- Bei, D., Meng, J., Youan, B.B., 2010. Engineering nanomedicines for improved melanoma therapy: progress and promises. *Nanomed. (Lond.)* 5 (9), 1385–1399.
- Blankenberg, S., Barbaux, S., Tiret, L., 2003. Adhesion molecules and atherosclerosis. *Atherosclerosis* 170 (2), 191–203.
- Borai, I.H., Ezz, M.K., Rizk, M.Z., Matloub, A.A., El-Sherbiny, M., Aly, H.F., Fouad, G.I., 2015. Hypolipidemic and anti-atherogenic effect of sulphated polysaccharides from the green alga *Ulva fasciata*. *Int. J. Pharm. Sci. Rev.* 31 (1), 1–12.
- Burrows, R., Collett, J.H., Attwood, D., 1994. The release of drugs from monoglyceride-water liquid crystalline phases. *Int. J. Pharm.* 111, 283–293.
- Clogston, J., Craciun, G., Hart, D.J., Caffrey, M., 2005. Controlling release from the lipidic cubic phase by selective alkylation. *J. Control Release* 102, 441–4461.
- Drury, R.A., Wallington, E.A., 1980. *Carleton's Histology Technique*. Oxford University Press, New York.
- Flock, M.R., Green, M.H., Kris-Etherton, P.M., 2011. Effects of adiposity on plasma lipid response to reductions in dietary saturated fatty acids and cholesterol. *Adv. Nutr.* 2, 261–274.
- Fossati, P., Prencipe, L., 1982. Serum triglycerides determined colorimetrically with an enzyme that produces hydrogen peroxide. *Clin. Chem.* 28 (10), 2077–2080.
- Gustafsson, J., Ljusberg-Wahren, H., Almgren, M., Larsson, K., 1997. Submicron particles of reversed lipid phases in water stabilized by a nonionic amphiphilic polymer. *Langmuir* 13, 6964–6970.
- Haag, R., Kratz, F., 2006. *Polymer therapeutics: concepts and applications*. *Angew. Chem. Int. Ed.* 45, 1198–1215.
- Han, J.M., Li, H., Cho, M.H., Baek, S.H., Lee, C.H., Park, H.Y., Jeong, T.S., 2017. Soy leaf extract exerts atheroprotective effects via modulation of Kruppel like factor 2 and adhesion molecules. *Int. J. Mol. Sci.* 18, 373.
- Hou, D., Xie, C., Huang, K., Zhu, C., 2003. The production and characteristics of solid lipid nanoparticles (SLNs). *Biomaterials* 24 (10), 1781–1785.
- Jang, A., Srinivasan, P., Lee, N.Y., 2008. Comparison of hypolipidemic activity of synthetic gallic acid, linoleic acid ester with a mixture of gallic acid and linoleic acid, gallic acid, and linoleic acid on high-fat diet induced obesity in C57BL/6 Cr Slc mice. *Chem. Biol. Interact.* 174, 109–117.
- Katiyar, V., Khare, R., Imran, P., 2016. Symptoms & diagnosis of fatty liver diseases in human beings. *IJERMDC* 38, 8–13.
- Korting, H.C., Schafer-Korting, M., 2010. Carriers in the topical treatment of skin disease. *Handbook Exp. Pharmacol.* 197, 435–468.
- Koter, M., Broncel, M., Chojnowska-Jezierska, J., Kliaczynska, K., Franiak, I., 2002. The effect of atorvastatin on erythrocyte membranes and serum lipids in patients with type-2 hypercholesterolemia. *Eur. J. Clin. Pharmacol.* 58 (8), 501–506.
- Langtry, H.D., Markham, A., 1999. Fluvastatin - a review of its use in lipid disorders. *Drugs* 57, 583–595.
- Lara, M.G., Bentley, M.V., Collett, J.H., 2005. In vitro drug release mechanism and drug loading studies of cubic phase gels. *Int. J. Pharm.* 293, 24–50.
- Li, B., Lu, F., Wei, X., Zhao, R., 2008. Fucoidan: structure and bioactivity. *Molecules* 13 (8), 1671–1695.
- Matloub, A.A., El-Sherbiny, M., Borai, I.B., Ezz, M.K., Rizk, M.Z., Aly, H.F., Fouad, G.I., 2013. Assessment of anti-hyperlipidemic effect of water soluble polysaccharides of *Ulva fasciata* delile on cholesterol-fed rats. *J. Appl. Sci.* 9, 2983–2993.
- Montgomery, H.A., Dymock, J.F., 1986. The determination of nitrate in water. *Analyst* 86, 414–415.
- Nasr, M., Ghorab, M.K., Abdelazem, A., 2015. In vitro and in vivo evaluation of cubosomes containing 5-fluorouracil for liver targeting. *Acta Pharm. Sin. B* 5 (1), 79–88.
- Nguyen, T.H., Hanley, T., Porter, C.J., Boyd, B.J., 2011. Nanostructured liquid crystalline particles provide long duration sustained-release effect for a poorly water soluble drug after oral administration. *Control Release* 153, 180–185.
- Paget, G.E., Barnes, J.M., 1964. *Evaluation of Drug Activities: Pharmacometrics*. Academic Press, London and New York.
- Pengzhan, Y., Ning, L., Xiguang, L., Gefei, Z., Quanbin, Z., Pengcheng, L., 2003. Antihyperlipidemic effects of different molecular weight sulfated polysaccharides from *Ulva pertusa* (Chlorophyta). *Pharmacol. Res.* 48 (6), 543–549.
- Rizk, M., Aly, H.F., Matloub, A.A., Fouad, G.I., 2016a. The anti-hypercholesterolemic effect of ulvan polysaccharide extracted from the green alga *Ulva fasciata* on aged hypercholesterolemic rats. *Asian J. Pharmaceut. Clin. Res.* 9, 165–176.
- Rizk, M., El-sherbiny, M., Borai, I.H., Ezz, M.K., Aly, H.F., Matloub, A.A., Farrag, A.E., Ghadha, I., Fouad, G.I., 2016b. Sulphated polysaccharides (SPS) from the green alga *Ulva fasciata* extract modulates liver and kidney function in high fat diet-induced hypercholesterolemic rats. *Int. J. Pharmacy Pharmaceut. Sci.* 8, 43–55.
- Rizwan, S.B., Dong, Y.D., Boyd, B.J., Rades, T., Hook, S., 2007. Characterisation of bicontinuous cubic liquid crystalline systems of phytantriol and water using cryo field emission scanning electron microscopy (cryo FESEM). *Micron* 38, 478–484.
- Sadhale, Y., Shah, J.C., 1999. Biological activity of insulin in GMO gels and the effect of agitation. *Int. J. Pharm.* 191, 65–74.
- Said, M.M., Ezz, M.K., Matloub, A.A., 2017. Protective effect of sulfated polysaccharide isolated from *Ulva fasciata* against galactosamine-induced liver injury in rats. *J. Food Biochem.* (e 12383)
- Salama, A.H., Aburahma, M.H., 2016. Ufasomes nano-vesicles-based lyophilized platforms for intranasal delivery of cinnarizine: preparation, optimization, ex-vivo histopathological safety assessment and mucosal confocal imaging. *Pharm. Dev. Technol.* 21 (6), 706–715.
- Salama, A.H., Mahmoud, A.A., Kamel, R., 2016. A novel method for preparing surface-modified fluocinolone acetonide loaded PLGA nanoparticles for ocular use: in vitro and in vivo evaluations. *AAPS PharmSciTech* 17 (5), 1159–1172.
- Scriven, L.E., 1976. Equilibrium bicontinuous structure. *Nature* 263, 123–124.
- Semete, B., Booyens, L., Lemmer, Y., Kalombo, L., Katata, L., Verschoor, J., Swai, H.S., 2010. In vivo evaluation of the biodistribution and safety of PLGA nanoparticles as drug delivery systems. *Nanomedicine* 6 (5), 662–671.
- Shah, M.H., Paradkar, A., 2005. Cubic liquid crystalline glyceryl monooleate matrices for oral delivery of enzyme. *Int. J. Pharm.* 294, 161–172.
- Souto, E.B., Wissing, S.A., Barbosa, C.M., Muller, R.H., 2004. Development of a controlled release formulation based on SLN and NLC for topical clotrimazole delivery. *Int. J. Pharm.* 278 (1), 71–77.
- Spicer, P., 2005. Cubosome processing industrial nanoparticle technology development. *Chem. Eng. Res. Des.* 83, 1283–1285.
- Suanarunsawat, T., Ayutthaya, W.D., Songsak, T., Thirawarapan, S., Pongshompo, S., 2011. Lipid-lowering and antioxidative activities of aqueous extracts of *Ocimum sanctum* L. leaves in rats fed with a high-cholesterol diet. *Oxidat. Med. Cell. Long.* 9.
- Ustyol, A., Aycan Ustyol, E., Gurdol, F., Kokali, F., Bekpınar, S., 2017. P-selectin, endocan, and some adhesion molecules in obese children and adolescents with non-alcoholic fatty liver disease. *Scand. J. Clin. Lab. Invest.* 77 (3), 205–209.
- Wang, S., Tan, M., Zhong, Z., Chen, M., Wang, Y., 2011. Nanotechnologies for curcumin: an ancient puzzler meets modern solutions. *J. Nanomater.* 2011, 8.
- Yang, Y., Chung, T., Bai, X., Chan, W., 2000. Effect of preparation conditions on morphology and release profiles of biodegradable polymeric microspheres containing protein fabricated by double-emulsion method. *Chem. Eng. Sci.* 55, 2223–2235.
- Yida, Z., Imam, M.U., Ismail, M., Ismail, N., Ideris, A., Abdullah, M.A., 2015. High fat diet-induced inflammation and oxidative stress are attenuated by N-acetylneuraminic acid in rats. *J. Biomed. Sci.* 22, 96.
- Zollner, N., Kirsch, K., 1962. On the quantitative determination of lipoids (micromethode) by means of the many natural lipoids (all known plasmalipids) common sulpho phospho vanillin reaction. *Z. Sat. Exp. Med.* 135, 545–560.